https://doi.org/10.5194/cp-2020-146
Preprint. Discussion started: 3 December 2020

Climate of the Past Discussions

Variations in mineralogy of dust in an ice core obtained from northwestern Greenland over the past 100 years

Naoko Nagatsuka[1], Kumiko Goto-Azuma[1, 2], Akane Tsushima[3], Koji Fujita[4], Sumito Matoba[5], Yukihiko Onuma[6], Moe Kadota[5, 7], Masahiro Minowa[4], Yuki Komuro[1], Hideaki Motoyama[1, 2], and Teruo Aoki[1]

[1] National Institute of Polar Research, Tokyo 190-8518, Japan
[2] Department of Polar Science, The Graduate University for Advanced Studies, SOKENDAI, Tokyo 190-8518, Japan
[3] Meteorological Research Institute, Tsukuba 305-0052, Japan
[4] Graduate School of Environmental Studies, Nagoya University, Nagoya 464-8601, Japan
[5] Institute of Low Temperature Science, Hokkaido University, Sapporo 060-0819, Japan
[6] Institute of Industrial Science, University of Tokyo, Kashiwa 277-8574, Japan
[7] Graduate School of Environmental Science, Hokkaido University, Sapporo 060-0810, Japan

Correspondence: Naoko Nagatsuka (nagatsuka.naoko@nipr.ac.jp)

Abstract. Our study is the first to demonstrate a high-temporal-resolution record of mineral composition in a Greenland ice core over the past 100 years. To reconstruct the past variations in the sources and transportation processes of mineral dust in northwestern Greenland, we analyzed the morphology and mineralogical composition of dust in an ice core from 1915 to 2013 using Scanning Electron Microscopy (SEM) and Energy-Dispersive X-ray Spectroscopy (EDS). Analysis of the SEM-EDS reveals that the ice core dust mainly consisted of silicate minerals and the composition varied substantially on multi-decadal and inter-decadal scales, suggesting that the geological origin of the ice core minerals changed periodically during the past 100 years. The multi-decadal variation trend differed among mineral types: kaolinite generally formed in low- or middle-latitude areas were abundant in the colder periods (1950 to 2000), whereas mica, chlorite, feldspars, mafic minerals, and quartzes formed in arid, high-latitude, and local areas were abundant in the warmer periods (1915 to 1949 and 2005 to 2013). This indicates that the multi-decadal variation of the relative abundance of the minerals can be attributed to the local temperature changes in Greenland. The trajectory analysis shows that the minerals were mainly transported from the western coast of Greenland in the two warming periods, which was likely due to an increase of dust sourced from local ice-free areas. On the other hand, the abundant kaolinite was likely derived from old sediments at higher latitudes in North America, rather than from low and middle latitudes.

1. Introduction

Aeolian mineral dust in snow and ice on the Greenland Ice Sheet provides key information about global and local climate change. Past dust deposition can be reconstructed from ice cores, and such records reveal substantial variations in the concentration, composition, particle size, and morphology of minerals. Ice core dust records show a close relationship with climate signals, such as temperature and atmospheric circulation. Dust concentrations in Greenland ice cores during the last glacial maximum were 40 times higher than those over the last 10,000 years, and were strongly correlated with temperature changes (as indicated by $\delta^{18}O$ records; e.g., de Angelis et al., 1997; Mayewski et al., 1997; Fuhrer et al., 1999; Schüpbach et al., 2018). Steffensen et al. (1997) also showed a systematic connection between dust volume distribution, total dust mass, and $\delta^{18}O$ in the Greenland Ice Core Project (GRIP) ice core, indicating that climate changes appear to have modified the processes of formation, transport, and deposition of the mineral dust in the same way over the last 120,000 years. The variability of ice core dust may be related to changes in atmospheric transport and dust source areas affected by climate change (Svensson et al., 2000). Thus, it is important to reconstruct the variations in the sources and transportation processes of mineral dust in ice cores.

https://doi.org/10.5194/cp-2020-146
Preprint. Discussion started: 3 December 2020

Climate of the Past Discussions

Geochemical analyses, such as the stable isotope ratio of Sr and Nd, have been used to identify possible sources of Greenland ice core dust. These isotopic ratios have strong regional variations that are controlled by their geological origins and rarely change during transportation in the atmosphere or after deposition. The isotope ratios of the GRIP and Greenland Ice Sheet Project 2 (GISP2) ice core dust obtained from 44 to 12 kyr B.P. indicated that possible source areas were eastern Asian deserts and the source areas varied little during the late Pleistocene (Biscaye et al., 1997; Svensson et al., 2000). Lupker et al. (2010) analyzed the Sr and Nd isotopic ratios of mineral dust in an ice core from southern Greenland (Dye 3) dating back to between 1786 and 1793 that revealed the Sahara Desert could be an additional dust source. However, these analyses have mostly targeted ice core dust from glacial periods characterized by a high dust concentration because Sr and Nd isotopic ratio analyses need large amounts of samples. Thus, there is limited information about possible sources of mineral dust in interglacial periods in which dust concentrations are low.

Scanning Electron Microscopy (SEM) and Energy-Dispersive X-ray Spectroscopy (EDS) are useful tools for revealing the source areas of samples with low amounts of mineral dust. SEM provides morphological information and EDS provides the mineralogical composition of individual particles, allowing the evaluation of the continental dust input and showing variations in ice core dust properties. Donarummo et al. (2003) analyzed the size distribution and mineral composition of GISP2 ice core dust during the 1930s by SEM-EDS and suggested that the central United States might have contributed a substantial amount of minerals to the ice core when the source area was affected by intense droughts. The SEM-EDS analysis of dust from snow pit samples from 1989 to 1991 at Summit in central Greenland indicated that the possible sources were likely to be Asian deserts and the source areas have not changed seasonally (Drab et al., 2002). Therefore, the SEM-EDS analysis reveals geological and temporal variations with high resolution in the mineral sources in ice cores during interglacial periods. However, the continuous variations of the dust properties in Greenland ice cores during recent years are still not well known.

Possible source areas for the Greenland ice core dust may have varied in recent years. Most of the Earth's surface has changed rapidly because of recent climate warming and human activities, which may result in changes in atmospheric transport and sources of mineral dust in the ice sheet. For example, a remarkable increase in dust outbreaks occurred recently in eastern Asian deserts, which are vast sources of eolian mineral dust, from 2000 to 2002 compared with the 1990s (Kurosaki and Mikami, 2003). The dust from the Asian deserts is transported to Greenland across the ocean. Furthermore, there may also be an increasing contribution of dust from local source areas in Greenland (Amino et al., 2020). The retreating ice and decreasing seasonal snow will expose more sediment in the proglacial area, delivering greater quantities of fine sediments to the floodplain than at present. Bullard and Austin (2011) reported that the exposure of the proglacial floodplain in Kangerlussuaq, western Greenland, during ice retreat may also make more material available for eolian transport. In this study, we describe the temporal variations in sources of minerals in an ice core obtained from the northwestern Greenland Ice Sheet covering a nearly 100-year-period (1915 to 2013) with a 5-year resolution. The morphology and mineralogical composition of the ice core dust were analyzed by SEM and EDS, and the variations are discussed in terms of changes in the ice core dust sources.

2. Samples and analytical methods

2.1 SIGMA-D ice core

The ice core was drilled at 2100 m a.s.l. in an accumulation area of the northwestern Greenland Ice Sheet called the SIGMA-D site (77.636° N, 59.120° W) in May 2014 (Matoba et al., 2015). The SIGMA-D site is located 250 km east of the town of Qaanaaq and lies in the upstream section of Heilprin Glacier, the largest outlet glacier in this area (Fig. 1). The ice core was recovered from the surface down to a depth of 222.72 m (total core length).

https://doi.org/10.5194/cp-2020-146
Preprint. Discussion started: 3 December 2020

Climate of the Past Discussions
Open Access
EGU

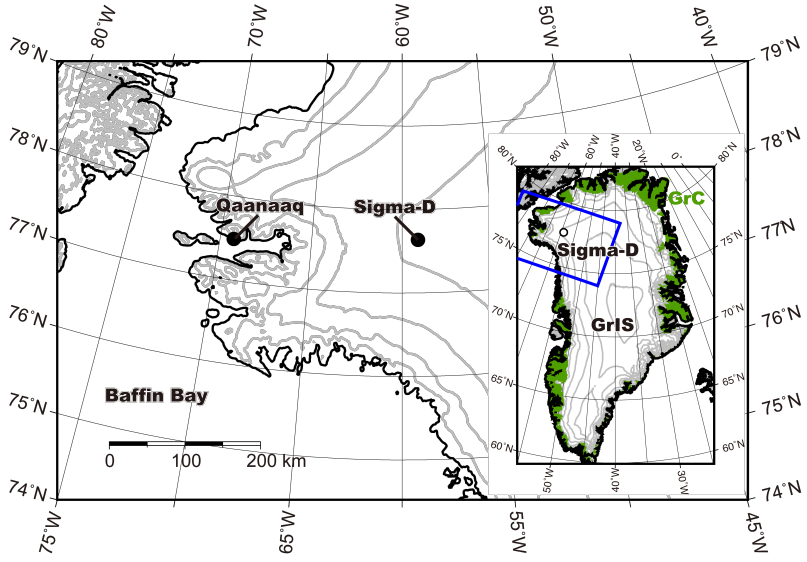

Figure 1. Location map of the SIGMA-D site (77.636°N, 59.120°W, 2100m a.s.l). Contour lines are drawn at a 500 m interval. The blue frame in the inset map of Greenland (GrIS) denotes the domain of the main map. The green shaded region in the inset map denotes the ice-free coastal terrain (GrC) used in the backtrajectory analysis.

2.2 Water isotope and ion concentration measurement

To determine the annual layers of the SIGMA-D ice core, the stable isotopes of water ($\delta^{18}O$) and the concentrations of sodium and sulfate ions (Na^+ and SO_4^{2-}) were measured at the Institute of Low Temperature Science, Hokkaido University, and the concentration of tritium was measured at the National Institute of Polar Research (NIPR), Tokyo, Japan.

The ice core samples were cut into 5–10 cm pieces with cross-sections of 30 cm^2 and decontaminated by removing the surface of each sample with a ceramic knife. Then, each sample was placed in a clean polyethylene bag and melted in a water bath, before being transferred to pre-cleaned polypropylene bottles in a tent for sample preparation at the field camp (Matoba et al., 2015). $\delta^{18}O$ was measured using a near-infrared cavity ring-down spectrometer (IR-CRDS, Picarro L2130-i, USA) with a high-throughput Picarro-A0212 vaporizer. The precision of determination was ±0.08 ‰ for $\delta^{18}O$. The concentrations of Na^+ and SO_4^{2-} were determined by ion chromatography (ICS-2100, Thermo Fisher Scientific, USA). Dionex AS-14A and CS-12A columns (Thermo Fisher Scientific) were used for anion and cation analyses, respectively. The limit of quantification was 5 ppb for both ions. For SO_4^{2-}, we also calculated its non-sea salt (nss) fractions as follows:

$$[\text{nss } SO_4^{2-}] = [SO_4^{2-}] - (SO_4^{2-} / Na^+)_{sea} \times [Na^+], \quad (1)$$

where $(SO_4^{2-} / Na^+)_{sea}$ is the mass ratio of SO_4^{2-} to Na^+ in the seawater, which is 0.252 (Wilson, 1975; Legrand and Mayewski, 1997). Tritium concentrations were measured using a liquid scintillation counter (LSC-LB3; Aloka Co. Ltd., Japan). The vertical resolution of the tritium measurements was 0.5 m.

2.3 SEM-EDS analysis of mineral dust

To extract mineral particles from the ice core at 5-year intervals, 4 -cm^2 cross-sections were cut from the 50-cm-long archived core sections in the −20 °C cold room at NIPR. The possibly contaminated outer layers (~1 cm thick) were removed using a pre-cleaned ceramic knife. Then, several millimeters of the ice surfaces were scraped off by the ceramic knife and collected in

https://doi.org/10.5194/cp-2020-146
Preprint. Discussion started: 3 December 2020

Climate of the Past Discussions

a clean 100-mL polyethylene bottle for every 5-year interval. The samples were freeze-dried at −45 °C using a freeze dryer (DRW240DA; Advantec, Japan) on a polycarbonate membrane filter (Advantec) with a diameter of 25 mm and pore size of 0.1 μm. The morphological characteristics and chemical composition of individual mineral particles on the membrane filter were observed by SEM (Quanta FEG 450, FEI) combined with EDS (X-Max 50, Oxford Instruments, UK) at NIPR. The filter targets were mounted on aluminum stubs using double-faced adhesive carbon tape and coated with vaporized platinum for SEM observation. In total, 150 particles were randomly chosen from the filter, and the equivalent circle diameter, the two-dimensional area (A), and the perimeter (P) were measured on digital photographs with an image-processing application (ImageJ, National Institutes of Health, USA). Then, the shape parameters of the particles were obtained, namely, circularity ($= (4\pi A) \times P^{-2}$). The major elemental composition (Na, Mg, Al, Si, Cl, S, Ca, K, Fe, P, and Ti) and related oxides (Na_2O, MgO, Al_2O_3, SiO_2, CaO, K_2O, Fe_2O_3, P_2O_5, and TiO_2) were obtained from the EDS spectra. The acceleration voltage and working distance for SEM analysis were 20 kV and 10 mm, respectively, and each EDS spectrum had more than 100,000 acquisition counts. To be counted as a mineral dust, a particle had to contain at least one of the elements Na, Mg, Si, Al, K, Ca, and Fe, each with an atomic ratio (%) amount at least twice that of the error (%). We did not count soluble particles, such as $CaSO_4$, Na_2SO_4, and NaCl, that can be derived from volcanic and marine aerosols.

2.4 Mineral identification

The mineralogical identification was performed using elemental composition and related oxides of individual mineral particles. Previous studies used protocols to semi-quantitatively identify the mineralogy of individual particles in ice cores by SEM-EDS analysis (e.g., Mudroch et al., 1977; Maggi, 1997; Donarummo et al., 2003; Wu et al., 2016). The identification of the SIGMA-D ice core dust followed three procedures (Wu et al., 2016). First, the spectrum pattern of each particle was matched to those of standard minerals (Severin, 2004). Second, we compared the oxide composition and morphology of the ice core dust with those of the standard minerals. Finally, a sorting scheme used to identify minerals in the GISP2 Greenland ice core dust by SEM-EDS was applied to identify the mineral types from the peak intensity ratios (Donarummo et al., 2003). Comparing the results of these procedures enables reliable mineral identification (Maggi et al., 1997; Wu et al., 2016).

Based on the formation process (weathering types), formation environment (temperature and humidity), and possible sources of the SIGMA-D ice core dust, most of the silicates we analyzed could be classified into the following five types. Type A consists primarily of kaolinite, which is a clay mineral generally formed by chemical weathering in warm and humid regions, including Africa, South America, and Southeast Asia (e.g., Mueller and Bocquier, 1986; Velde, 1995; Bergaya et al., 2006). We also find a mineral composed of Si and Al, but with a higher proportion of Si and a lower proportion of Al compared with kaolinite. It is likely pyrophyllite, which is generally found with kaolinite, and is thus also classified as Type A. Type B comprises mica, chlorite, and a mixture of the two, which are clay minerals formed by mechanical weathering of igneous and metamorphic rocks in cold and dry regions (e.g., Cremaschi, 1987; Pye, 1987; Velde, 1995). Type C consists of feldspars (Na/Ca-plagioclase and K-feldspar), which are also formed by mechanical weathering in cold and dry regions (e.g., Nahon, 1991). Type D comprises mafic minerals containing abundant Mg and Fe, such as hornblende and pyroxene, which are less frequent in atmospheric dust and are formed by mechanical weathering (e.g., Deer et al., 1993). Type E consists of quartzes, which are the most physically and chemically resistant minerals to weathering and their abundance in the atmosphere is related to the large desert source areas (Genthon and Armengaud, 1995; Pye,1987; Yokoo et al., 1994). According to previous studies, some minerals have localized distributions. Ito and Wagai (2017) showed the global terrestrial distribution of clay size mineral groups, revealing that Type A minerals were predominant in humid regions in low- or middle-latitude areas, whereas Type B minerals were abundant in arid and/or high-latitude areas. Furthermore, kaolinite (Type A) can be used as an indicator of intensive weathering in paleoclimatic conditions (Biscaye et al., 1965; Griffin et al., 1968). For example, the relative abundance of kaolinite (Type A) to chlorite (Type B) is a mineral indicator that is most sensitive to latitude dependency. The kaolinite/chlorite ratio shows higher values for minerals from low latitudes, such as North Africa, but showed lower values for

https://doi.org/10.5194/cp-2020-146
Preprint. Discussion started: 3 December 2020

Climate of the Past Discussions
Open Access
EGU

minerals from the northern hemisphere, such as Asia and North America (e.g., Biscaye et al., 1997; Maggi et al., 1997; Svensson et al., 2000; Donarummo et al., 2003). This trend reflects a decrease in weathering intensity with latitude. In addition to variations in kaolinite and chlorite, Type C, D, and E minerals also reflect the geological and climatic conditions of their source areas, as mentioned above. Thus, compositional variations among the five types of minerals can be used as an indicator of the source and transportation process of ice core dust in different periods. In this study, we consider each type of mineral as possibly being contributed from the following sources: Type A, low-middle latitude areas (e.g. Central Africa, South America, Southeast Asia); Types B and C, high-latitude (e.g. North America, Russia, North Europe) and/or desert areas (e.g. Asia and North Africa); Type D, local areas (Greenland); Type E, desert areas (e.g. Asia and North Africa).

2.5 Backward trajectory analysis

To investigate the possible source regions of the ice core dust, the air mass transport pathways are analyzed using the Hybrid Single-Particle Lagrangian Integrated Trajectory (HYSPLIT) model, which is distributed by National Oceanographic and Atmospheric Administration (NOAA, Stein et al., 2015). Points at 50 and 500 m above ground level (a.g.l.) at the SIGMA-D site are set as the initial points of an air mass for the 7-day backward trajectories. The probability distribution of the air mass at altitudes below 1,500 m a.g.l. is calculated at a 1° resolution. We assumed wet deposition for the preserved aerosol tracers (Iizuka et al., 2018; Parvin et al., 2019), and thus the probability was weighted by the daily precipitation when the air mass arrived at the ice-core site. We used daily precipitation from the ERA-40 and ERA-Interim reanalysis data sets, both of which are produced by the European Centre for Medium-Range Weather Forecasts (Dee et al., 2011; Uppala et al., 2005). The daily precipitation of ERA-40 (p_{40}) was calibrated with that of ERA-Interim (p_{int}) via a linear regression obtained for the period of 1979–2001 (p_{int}=0.47p_{40}, $R^2 = 0.702$, $p < 0.001$) to maintain consistency between the two precipitation datasets for the entire period (1958–2014). We also calculated the regional contribution from the probability distribution, for which land regions were divided into the following 5 regions: the Greenland ice sheet, the Greenland coast, Canada, northern Eurasia, and China (Fig. 2a).

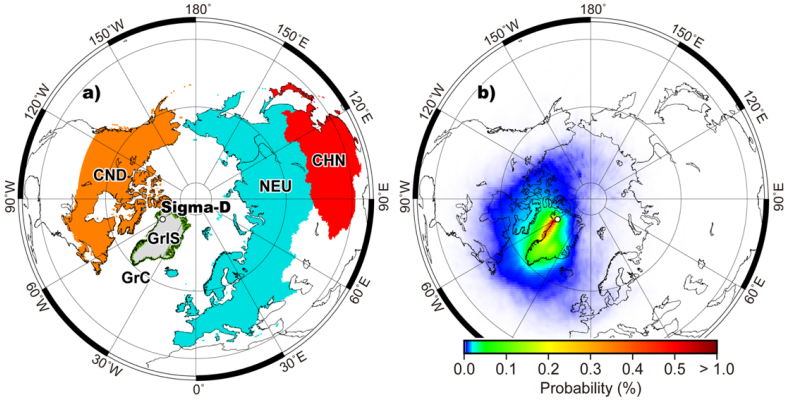

Figure 2. Map showing (a) the location of the SIGMA-D (Sigma-D) ice core site in Greenland and five regions for calculating regional contribution (GrIS: Greenland ice sheet (grey), GrC: Greenland coast (green), CND: Canada (orange), NEU: northern Eurasia (blue), CHN: China (red)) and (b) the probability distribution of an air mass at the SIGMA-D site from a 7-day three-dimensional backward-trajectory analysis during 1958 to 2014.

https://doi.org/10.5194/cp-2020-146
Preprint. Discussion started: 3 December 2020

Climate of the Past Discussions
Open Access
EGU

2.6 Snow cover fraction

To examine the surface condition of neighboring source for mineral dust emission, we analyzed inter-annual changes in snow cover fraction derived from multiple numerical simulations by a climate model. Various international organizations have conducted many numerical experiments simulated with global climate models to reproduce or predict climate change from past to future. The experiment products have been published by Coupled Model Intercomparison Project Phase 6 (CMIP6, Eyring et al., 2016) under the auspices of the World Climate Research Programme (WCRP). In this study, snow cover fraction derived from historical simulations from 1850 to 2014 (Onuma and Kim, 2020a, b, c, d) were used to examine mineral dust sources for SIGMA-D. The dataset was produced by MIROC6, a climate model developed by a Japanese modelling community (Tatebe et al., 2019), with four reanalysis datasets such as GSWP3 (Kim, 2017), CRUJRA (Harris, 2019), Princeton (Sheffield et al., 2006), and WFDEI (Weedon et al., 2014) as meteorological conditions in Land Surface, Snow and Soil moisture Model Intercomparison Project (LS3MIP, van den Hurk et al., 2016), which is a branch project in CMIP6. We obtained inter-annual changes in snow cover fraction during summer in the northwest- and southwest-coasts of Greenland (boundary at 70° N).

Table 1. Description of the SIGMA-D ice core dust samples

Period	Ice		Dust (size)		
	Top (m)	Bottom (m)	Average (μm)	Maximum (μm)	Log-normal Mode (μm)
1915−1919	37.00	38.60	2.00	12.80	0.73
1920−1924	35.49	37.00	2.60	16.30	1.15
1925−1929	33.80	35.49	2.20	26.50	0.46
1930−1934	31.85	33.80	1.60	12.10	0.58
1935−1939	30.22	31.85	2.30	20.10	0.59
1940−1944	28.57	30.22	1.70	15.00	0.59
1945−1949	26.87	28.57	2.60	21.80	0.97
1950−1954	25.02	26.87	1.50	12.80	0.55
1955−1959	23.67	25.02	2.02	14.10	0.75
1960−1964	21.89	23.67	1.24	6.70	0.60
1965−1969	19.95	21.89	1.31	9.60	0.53
1970−1974	17.85	19.95	0.97	4.94	0.35
1975−1979	16.30	17.85	1.02	5.50	0.43
1980−1984	14.61	16.30	1.90	11.90	0.58
1985−1989	12.50	14.61	1.20	5.50	0.47
1990−1994	10.03	12.50	2.20	15.90	0.68
1995−1999	7.56	10.03	2.08	14.86	0.77
2000−2004	4.62	7.56	1.45	8.70	0.65
2005−2009	2.31	4.62	1.86	11.29	0.60
2010−2013	0.00	2.31	2.03	25.95	0.51

https://doi.org/10.5194/cp-2020-146
Preprint. Discussion started: 3 December 2020

Climate of the Past Discussions
Open Access
EGU

3. Results

3.1 Dating of the SIGMA-D ice core

Dating of the SIGMA-D ice core, which was performed by annual layer counting of $\delta^{18}O$ and Na^+, showing obvious seasonal variations (Fig. A1). The observed seasonality of chemical components and the water stable isotope ratio in the snowpack and ice cores has previously been reported at various sites on the Greenland Ice Sheet (Whitlow et al., 1992; Legland and Mayewski, 1997; Kuramoto et al., 2011; Oyabu et al., 2016; Kurosaki et al., 2020). The winter season of the SIGMA-D ice core was defined as the depth at which $\delta^{18}O$ was at its minimum value and Na^+ was at its maximum value, and we counted winter season to winter season as 1 year.

Other fixed dates were provided by the tritium profile and $nssSO_4^{2-}$ spikes. A sharp tritium peak at 11.56 m w.e. corresponds to the H-bomb test in 1963 (Koide et al., 1982, Clausen and Hammer, 1988), indicating an accumulation rate of 0.23 m w.e. yr^{-1} from 1963 to 2013. The large $nssSO_4^{2-}$ peak appeared at 54.17 m w.e. is assumed to correspond to the eruption of the Laki volcano in 1783. The $nssSO_4^{2-}$ signal of the 1783 Laki eruption has also been found in other ice cores in Greenland, Arctic Canada, and Svalbard (Clausen and Hammer, 1988; Grumet et al., 1998; Matoba et al., 2002). Similarly, we assume other $nssSO_4^{2-}$ spikes to be the signatures of unknown (1810), Tambora (1816), and Katmai (1912) volcanic eruptions at shallower depths of 47.53, 46.03, and 23.50 m w.e., respectively. Comparing the annual layer counting and these reference horizons, we estimate that the ice core dating includes a 1-year error.

As a result of these analyses, we estimate that the upper 112.87 m (86.06 m w.e.) of the ice core is equivalent to the period from 1660 to 2013. In this study, we used ice samples to a depth of 38.60 m (22.75 m w.e.) covering 1915 to 2013 for the SEM and EDS analyses (Table 1).

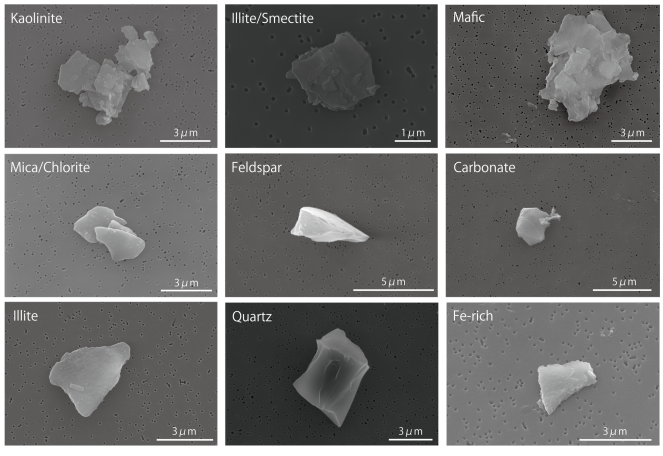

Figure 3. SEM images of each mineral group in the SIGMA-D ice core.

3.2 Particle morphology

Figure 3 shows SEM images of the mineral dust in the SIGMA-D ice core. The number size distribution of mineral dust in the SIGMA-D ice core showed that most particles had a diameter of <2 μm (Fig. 4), which is consistent with other Greenland ice core dust (e.g., Steffensen, 1997; Biscaye et al., 1997). The mean and maximum particle diameters, calculated as 5-year averaged values, ranged from 0.97 to 2.60 μm and 4.94 to 26.51 μm, respectively, with a single modal structure at the peak

https://doi.org/10.5194/cp-2020-146
Preprint. Discussion started: 3 December 2020

Climate of the Past Discussions
Open Access
EGU

ranged from 0.35 to 1.15 μm. The size distribution varied among the samples collected from different periods, showing a narrower peak with finer mode (0.35–0.53 μm) for the samples from 1965 to 1979 and a broader peak with a coarser mode for the samples from 1920 to 1924 and 1945 to 1949 (0.97–1.15 μm; Figure A2). There were coarser particles with diameters of >10 μm in the samples from 1915 to 1959 and from 1990 to 2013, but no particles with diameters of >10 μm were found in the samples from 1960 to 1989, except for the sample from 1980 to 1984.

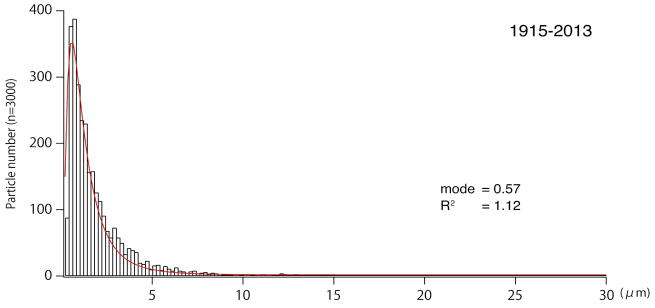

Figure 4. Particle size distribution and log-normal fitting results (mode: mode diameter and R2: half peak width) of minerals in the ice core samples during 1915 to 2013.

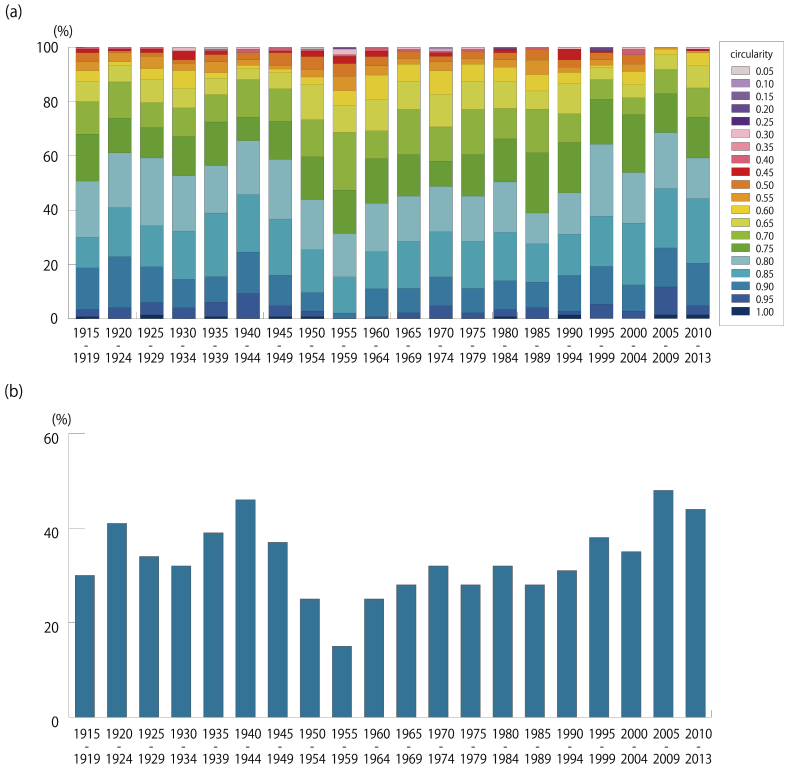

Figure 5. (a) Circularity distribution of mineral particles from different period. (b)Variation in proportion of circularity values of >0.8

https://doi.org/10.5194/cp-2020-146
Preprint. Discussion started: 3 December 2020

Climate of the Past Discussions
Open Access
EGU

3.3 Quantitative estimation of mineral dust

The elemental composition of individual mineral particles obtained from the EDS analysis showed that the ice core dust was composed mainly of silicate minerals in all the samples (65%–95%, Fig. 6). Based on a peak intensity ratio sorting scheme (Donarummo et al., 2003) and comparison of oxide composition and morphological information with those of standard minerals, the silicates were categorized as quartz, Na/Ca- and K-feldspars, clays (kaolinite, pyrophyllite, smectite, illite, micas, and chlorite, as well as mixed layers of illite/smectite and mica/chlorite), and mafic minerals rich in magnesium and iron (Figs. 3 and 7). These minerals were also found in Greenland ice cores from glacial periods (e.g., Maggi, 1997; Svensson et al., 2000). Semi-quantitative analysis of the EDS-spectrum showed that the proportion of kaolinite among 150 mineral particles found in each sample was the highest (5%–66%) and that of smectite was the lowest (0%–2%) in nearly every period (Fig. 7 and Table 2). The proportion of pyrophyllite, mica/chlorite-mix, quartz, feldspars, and illite/smectite-mix was the second highest, varying from 6%–25%, 3%–25%, 3%–22%, 1%–20%, and 0%–13%, respectively. The mineralogy of the SIGMA-D ice core dust showed significantly higher kaolinite contents compared with those of the other Greenland ice cores (GRIP, 4%–16% (Svensson et al., 2000); GISP2, 0%–2% (Donarummo et al., 2003)).

The silicate mineral composition showed large variations among the samples on two different time scales. First, the compositions varied on a multi-decadal scale, with higher kaolinite and pyrophyllite contents (30%–67% and 7%–26%) and lower mica/chlorite-mix contents in the 1950 to 2004 samples (3%–9%, 1%–13%, and 5%–15%, respectively), especially in the 1970 to 2004 samples. The opposite trend was observed in the 1915 to 1949 and 2005 to 2013 samples (kaolinite and pyrophyllite: 5%–20% and 6%–16%, respectively; mica/chlorite-mix: 10%–25%). The compositional variation also showed higher feldspars, mafic, and quartz contents in the 1915 to 1945 and 1990 to 2013 samples (feldspars: 1%–20%; mafic: 0%–9%; quartz: 10%–22%) than in the other periods (feldspars: 3%–6%; mafic: 1%–2%; quartz: 3%–6%). Second, the compositions varied on shorter time scales, in inter-decadal cycles. Variations in the compositions of feldspars, micas, chlorite, and mica/chlorite-mix were similar, but opposite to those of kaolinite and pyrophyllite.

Non-silicate minerals were also found in the ice core samples and were mainly composed of Ca- and Fe-dominant minerals, identified as carbonates (calcite) and Fe-oxides (pyrite, magnetite, or hematite), respectively (Fig. 6). The relative abundance of both minerals, ranging from 0% to 15%, increased in recent 10 years. The carbonate minerals showed the highest abundance in the 1960–1964 sample.

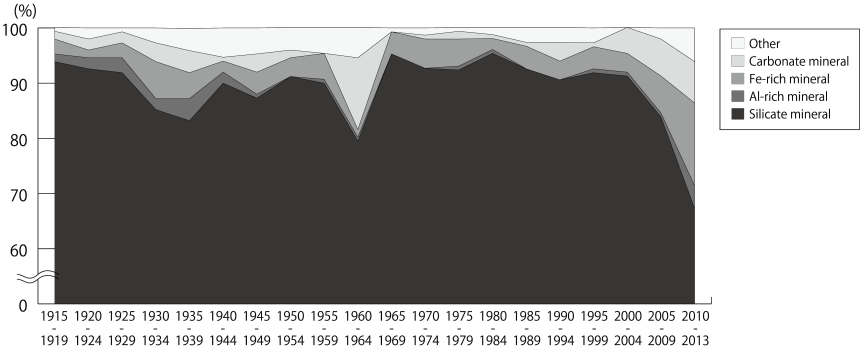

Figure 6. Variations of the insoluble mineral records in the ice core dust in 5-year resolution.

https://doi.org/10.5194/cp-2020-146
Preprint. Discussion started: 3 December 2020

Climate of the Past Discussions
Open Access
EGU

Table 2. Relative abundance (%) of silicate mineral groups for each sample.

Sample Period	Kaolinite	Pyro-phyllite	Smectite	Illite/ Smectite	Illite	Micas	Micas/ chlorite	Chlorite	Na/Ca-feldspar	K-feldspar	Mafic	Quartz	Un-known
1915-1919	17.7	15.6	0.0	6.4	8.5	1.4	9.2	5.0	7.1	6.4	5.0	14.9	2.8
1920-1924	18.8	2.9	2.2	5.1	4.3	3.6	22.5	2.9	4.3	6.5	2.2	20.3	4.3
1925-1929	19.7	10.2	0.7	4.4	2.9	4.4	21.9	4.4	4.4	0.7	8.8	13.1	4.4
1930-1934	19.7	15.0	2.4	5.5	0.0	4.7	25.2	4.7	3.1	0.0	0.8	13.4	5.5
1935-1939	13.7	15.3	2.4	15.3	2.4	8.1	10.5	1.6	4.0	0.8	4.8	14.5	6.5
1940-1944	16.3	7.4	0.0	5.9	3.7	4.4	16.3	5.2	3.7	1.5	3.7	22.2	9.6
1945-1949	21.4	7.6	0.8	10.7	3.1	1.5	13.0	6.1	14.5	3.8	4.6	9.9	3.1
1950-1954	38.8	20.9	0.7	11.2	0.0	2.2	6.7	3.7	3.0	0.0	0.7	5.2	6.7
1955-1959	31.1	16.3	0.7	14.1	2.2	6.7	9.6	5.9	3.0	0.0	3.7	3.7	3.0
1960-1964	37.9	21.6	0.9	12.1	2.6	0.0	8.6	0.9	3.4	0.9	0.9	3.4	6.9
1965-1969	35.0	13.3	0.0	13.3	2.8	0.7	11.9	1.4	4.2	1.4	2.1	5.6	8.4
1970-1974	30.2	7.2	0.7	4.3	1.4	2.2	15.1	11.5	2.9	2.9	1.4	5.8	14.4
1975-1979	58.6	12.8	0.0	6.8	3.0	1.5	3.0	0.8	3.8	0.0	0.8	5.3	3.8
1980-1984	66.7	4.9	0.0	3.5	0.7	4.2	4.2	0.7	2.8	2.1	2.1	2.8	5.6
1985-1989	40.1	26.3	0.7	8.0	0.7	1.5	7.3	1.5	3.6	0.7	0.0	5.1	4.4
1990-1994	39.2	20.0	0.7	5.9	0.7	0.0	2.2	4.4	10.4	0.7	2.2	8.9	4.4
1995-1999	44.5	7.3	1.5	3.6	2.9	0.7	5.1	1.5	9.5	2.9	8.0	5.1	7.3
2000-2004	62.5	12.5	0.0	2.2	2.9	0.7	5.9	1.5	0.7	0.0	0.0	8.1	2.9
2005-2009	4.8	5.6	1.6	3.2	10.4	2.4	20.8	8.8	12.8	7.2	3.2	10.4	8.8
2010-2013	10.1	10.1	0.0	7.1	7.1	2.0	14.1	5.1	12.1	5.1	5.1	11.1	10.1

https://doi.org/10.5194/cp-2020-146
Preprint. Discussion started: 3 December 2020

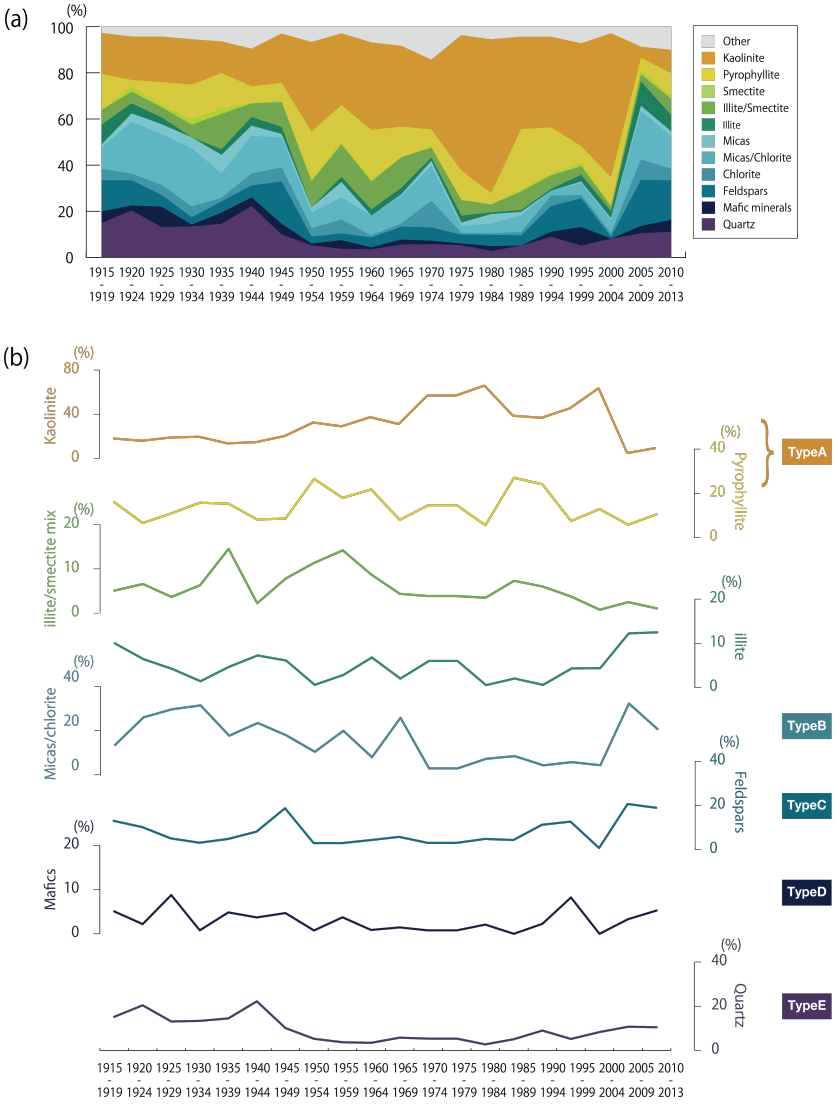

Figure 7. Variations of the silicate mineral records in the ice core dust in 5-year resolution. (a) mineral composition and (b) proportion of each mineral. Micas and chlorite composed of micas, mica/chlorite-mix, chlorite, and feldspars composed of Na/Ca-feldspar and K-feldspar.

3.4 Source regions of SIGMA-D ice core dust

To identify the source regions of the ice core dust, we applied the HYSPLIT back trajectory model and calculated the probability distributions of an air mass arriving at the SIGMA-D site from 1958 to 2014 (Figs. 2b and 8). The results show that the air mass at elevations above ground level from 0 to 1500 m came mainly from the western coast of Greenland, including the Baffin Bay, whereas a smaller part came from northern Canada (Figs. 2b and 8a). Excluding the ice sheet and ocean areas that could not be possible sources of mineral dust, the air mass is considered to have come mainly from the Greenland coast (50%–60%) and Canada (~40%), with a small contribution from northern Europe (~3%, Fig. 8b). Contributions from these three possible source regions show little seasonal and inter-annual variabilities (Fig. 8b and c).

https://doi.org/10.5194/cp-2020-146
Preprint. Discussion started: 3 December 2020

Climate of the Past Discussions
Open Access
EGU

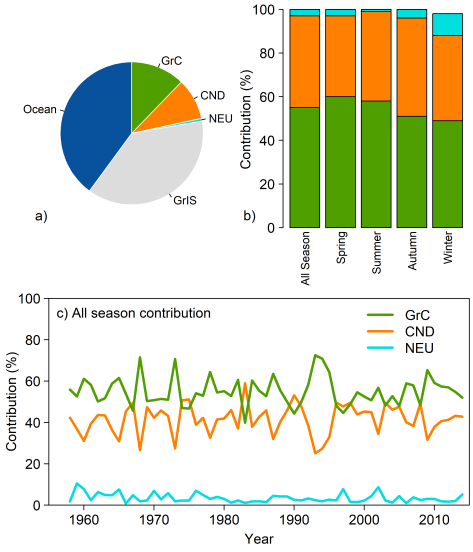

Figure 8. (a) Contribution rate of an air mass from possible source areas during 1958 to 2013. (b) Seasonal and (c) annual variations in the regional contribution of air mass to the SIGMA-D site excluding the ice sheet and ocean areas. GrC, GrIS, CND, NEU denote ice-free Greenland coastal region (Fig. 1), Greenland Ice Sheet, Canada, and northern Eurasia, respectively (Fig. 2a).

4. Discussion

4.1 Variation in silicate mineral composition

The SEM-EDS analysis revealed that the SIGMA-D ice core dust samples collected from 1915 to 2013 mainly contained silicate minerals, which is the most abundant family of crustal minerals (Deer et al., 1993). Silicate mineral composition showed variations on a multi- and inter-decadal scale, indicating that the geological origin of the minerals changed cyclically over two different time scales during the past 100 years.

Variation trends in the silicate mineral composition of the SIGMA-D ice core samples substantially differed among mineral types (Fig. 9), indicating that the minerals in the ice core were derived from multiple geological sources. The dominance of Type A minerals in the samples from 1950 to 2004 indicated that the minerals might be mainly derived from low- or middle-latitude areas in the periods. In contrast, the abundance of Type B, C, D, and E minerals in the samples from 1915 to 1949 and from 2005 to 2013 indicated that the minerals were likely derived from arid deserts and/or high latitude areas, including Greenland.

The morphological characteristics of the ice core dust also support the changes in the sources of silicate minerals. The size distribution of the minerals showed lower mean, maximum, and modal diameters from 1950 to 1994 compared with the other periods, when the samples comprised mainly Type A minerals (Table 1, Fig. A2). The circularity also showed a similar trend, containing smaller amounts of particles with circularity values >0.80 from 1950 to 1994 (Fig. 5). The particle size depended on the mineralogy of the ice core dust. The coarser fraction (>2 μm) of the ice core dust samples contained little clay, especially for the Type A minerals (Fig. 10), but contained an abundance of Type C, D, and E minerals. This particle size dependence is

https://doi.org/10.5194/cp-2020-146
Preprint. Discussion started: 3 December 2020

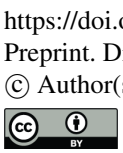

Climate of the Past Discussions
Open Access
EGU

260 consistent with other analyses of Greenland ice core dust (Biscaye, 1965; Svensson et al., 2000). Thus, the ice core dust was likely derived from different geological sources in the late 1990s compared with the other periods.

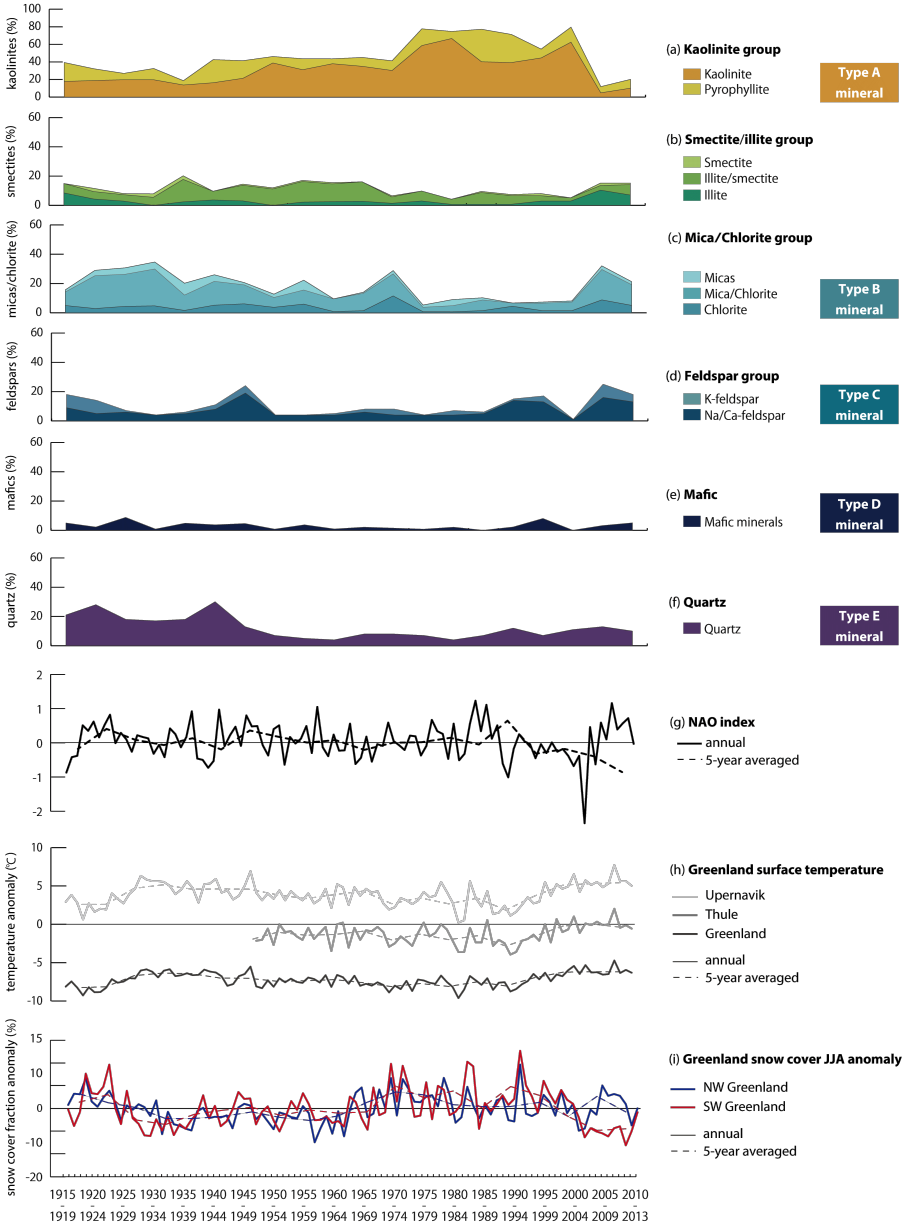

Figure 9. Comparison of historical changes in proportion of silicate minerals from the SIGMA-D ice core (a-f, a: kaolinite group, b: smectite group, c: mica/chlorite group, d: feldspar group, e: mafic mineral, f: quartz) with those in (g) North Atlantic Oscillation index (NAO, Hurrell and National Center for Atmospheric Research Staff, 2020), and (h) surface temperature anomalies and (i) snow cover fraction anomalies in Greenland, respectively. Surface temperature anomalies are deviation from 1948-2013 average in Thule. Temperature record of Greenland is from the Berkeley Earth and Thule (Pittufik) and Upernevik in western Greenland located 100km south and 650 km southeast of Qaanaaq are from Cappelen (2019). Snow cover fraction anomalies are deviation from 1915-2013 average in NW- and SW- Greenland, respectively.

https://doi.org/10.5194/cp-2020-146
Preprint. Discussion started: 3 December 2020

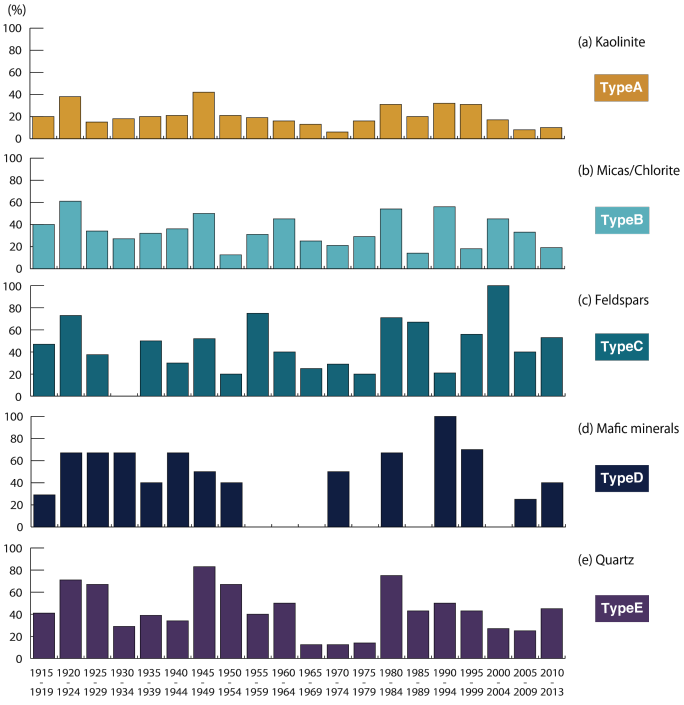

Figure 10. Historical changes in proportion of large particles (diameter >2μm) in (a) kaolinite, (b) mica/chlorite, (c) feldspars, (d) mafic minerals, and (e) quartz, respectively.

4.2 Possible causes of mineralogical variation

One of the possible causes of the temporal variations in the silicate mineral composition is a surface temperature change in Greenland. Reconstructions of temperature variability in Greenland have revealed there were two intense warming periods (the 1920s to 1940s and since the 1990s) and a cooling period (the 1950s to 1980s) in the past 100 years (e.g., Box et al., 2009; Kobashi et al., 2011; Cappelen, 2019). These trends were strong in the western coastal region and were similar to those of the silicate mineral compositions. The proportion of Type A minerals was low in the samples from 1915 to 1949, increased from 1950 to 2004, and decreased again after 2005. In contrast, the proportion of Type B, C, D, and E minerals showed the opposite trend. Therefore, Type A minerals were abundant in the colder periods, whereas Type B, C, D, and E minerals were abundant in the warmer periods (Fig. 9). These results suggest that the multi-decadal variation in the SIGMA-D ice core silicates can be attributed to the local temperature changes in Greenland.

The North Atlantic Oscillation (NAO) is also thought to be a possible cause of compositional variations in the silicate minerals. The NAO is known to show inter-decadal variations and is strongly related to the incidence and intensity of blocking high pressure over Greenland (Woollings et al., 2010; Hanna et al., 2014). Thus, the NAO can change the atmospheric circulation patterns and transportation processes associated with the ice core dust, which could be related to inter-decadal variations in the silicates. However, there is no clear correlation between the NAO and silicate mineral records. One of the reasons for this may be the low sampling resolution, which makes it difficult to determine a correlation with the NAO index.

In addition to the NAO, sulfate aerosols originating from volcanic eruptions have also been identified as another important cause of the cooling in Greenland, especially along the western ice sheet margins during the 1900s (Box et al., 2009), such as the Mt. Agung eruption in 1963, the Mt. St. Helens eruption in 1980, and the Mt. Pinatubo eruption in 1991. However, the

https://doi.org/10.5194/cp-2020-146
Preprint. Discussion started: 3 December 2020


Climate of the Past Discussions

chemical compositions of ash from these volcanoes (Taylor and Lichte, 1980; Pallister et al., 1992; Devi et al., 2019) were different from the composition of the Type A minerals that were abundant in the cooling period. The SEM observations also did not identify ice core minerals exhibiting morphological characteristics of volcanic ash. These results indicate that the effect of volcanic materials on the variation in the silicate mineralogy may be negligible in the SIGMA-D ice core.

4.3 Possible sources for mineral dust in the SIGMA-D ice core

The trajectory analysis revealed that the majority of the air mass came from the western coast of Greenland and that a smaller proportion came from northern Canada between 1958 and 2014. The contribution from these two possible source regions showed little inter-annual variabilities (Fig. 8b and c), indicating that the transportation processes of the ice core dust have not substantially changed on an annual basis over the last five decades. Thus, the variations in the geological origins of the ice core dust were unlikely due to changes in air mass transportation. An alternative cause of dust variability could be a change in the surface conditions of the source areas. Retreats of the ice sheet and local glaciers have accelerated since 2000 in Greenland, increasing the exposure of the ground surface in snow/ice-covered areas in the coastal region (e.g., van den Broeke et al., 2009; Bendixen et al., 2017). Furthermore, the modeled snow cover fraction anomaly during summer (June, July, and August) in northwest- and southwest- coasts of Greenland are negatively consistent with the temperature anomalies (Figs. 9h and 9i). The snow cover fractions are lower during the two warming periods from 1925 to 1960 and from 1990 to 2013. Since the snow cover fraction should directly relate to the snow cover duration, this result suggests that the snow cover duration in the west coast of Greenland was shortened for the warming periods and thus may also have contributed to the increase in local dust emissions. Bullard and Mockford (2018) analyzed records of dust events in the western Greenland coastal region and revealed that the annual severity of dust emissions was higher from 2000 to 2010 than during the preceding decades. This was likely due to increasing meltwater runoff delivering sediments from the ice sheet to outwash plains with the increase in atmospheric temperature. High dust emissions on the western coast of Greenland occurred in spring and summer, when the snow cover is rapidly decreasing (Bullard and Mockford, 2018). Our trajectory analysis also indicated that the air mass contribution from the Greenland coast was slightly larger in spring and summer than in autumn and winter (Fig. 8b). Therefore, the snow/ice cover duration in the Greenland coastal region was shortened by the recent warming during the melt season, causing an increase in the local supply of dust to the SIGMA-D site. Although no satellite observations are available for the first warming period (1920s to 1940s), aerial photos, maps, and paintings indicated ice retreat in Greenland (Box and Herrington, 2007). Thus, the abundant Type B, C, D, and E minerals found in the two warming periods were likely due to an increase of dust sourced from local ice-free areas.

Previous studies indicated dust transport from distant deserts, such as those in Asia and Africa, which are another possible source for three of the mineral types (B, C, and E) found at high elevation sites on the Greenland Ice Sheet. However, our trajectory analysis showed little contribution from these regions in the 7-day back trajectory. A similar analysis of an ice core in southeastern Greenland suggested that air mass contribution from Asian regions was negligible, even for the 25-day back trajectory (Iizuka et al., 2018).

The SEM-EDS analysis also indicated a contribution from local sediments in the warming periods. Compared with the silicate mineral composition of the GRIP ice core, which was derived mainly from Asian and African deserts, those of the SIGMA-D ice core showed a significantly lower proportion of Type E minerals (GRIP, 28%–44%, Svensson et al., 2000; SIGMA-D, 3%–22%), which has been recognized as an indicator of aeolian dust from eastern Asian deserts (Rex and Goldberg, 1958). The abundance of Type E minerals is related to the weathering of quartz-rich rocks as well as the large desert source areas in the world (Pye, 1987; Yokoo et al., 2004). The higher proportions of Type C and E minerals in the SIGMA-D ice core samples from 1915 to 1949 and from 1990 to 2013 correspond to higher concentrations of the two minerals in the surface dust and soil on and around the Qaanaaq Glacier (Nagatsuka et al., 2014). Thus, very little of the mineral dust in the SIGMA-D may have come from distant deserts, whereas a large proportion come from the local area in the warming periods.

https://doi.org/10.5194/cp-2020-146
Preprint. Discussion started: 3 December 2020

The low air mass contribution from low and middle latitudes indicated by the back trajectory analysis suggests that there are other possible sources for the abundance of Type A minerals found in the cooling period (1950s to 1980s). Type A minerals are typical of humid tropical climatic zones, such as those found in modern-day Africa and Southeast Asia (e.g., Bergaya et al., 2006). However, some studies have shown that other possible sources of Type A minerals are ancient soils formed by chemical weathering in high-latitude areas in past warming events. Darby (1975) analyzed the clay mineral composition of marine sediments from deep-sea cores in the Arctic Ocean and revealed that there was abundant kaolinite (Type A minerals) apparently derived from shale and soils of northern Alaska and northern Canada, which were relict deposits of warmer climates in the Tertiary. These abundant kaolinites were deposited in a non-marine environment (Allen and Johns, 1960). Clay mineralogy of North Sea Basin sediment cores also revealed that increased kaolinite concentrations were associated with Palaeocene-Eocene Thermal Maximum (Kemp et al., 2016). However, the mineralogical composition showed small amounts of kaolinite in the soil around the Qaanaaq Glacier in northwestern Greenland (Nagatsuka et al., 2014). Thus, the Type A minerals in the SIGMA-D ice core were likely transported from old sediments at higher latitudes in North America, rather than from low and middle latitudes and the local area.

5. Conclusions

Analysis of the SEM-EDS of individual dust morphology and mineralogy in the SIGMA-D ice core revealed that the ice core dust mainly consisted of silicate minerals, including quartz, feldspars, and mafic minerals, and clay minerals, including kaolinite, illite, smectite, micas, and chlorite. Most of the particles had a diameter of <2 μm, implying that the ice core contained mainly long-range transported wind-blown mineral dust. The silicate mineral composition varied substantially on multi-decadal and inter-decadal scales. The multi-decadal variation trend differed among mineral types formed in different source areas, which corresponded to that of the surface temperature change in Greenland: kaolinite generally formed in low- or middle-latitude areas were abundant in the colder periods (1950 to 2000), whereas mica, chlorite, feldspars, mafic minerals, and quartzes formed in arid, high-latitude, and local areas were abundant in the warmer periods (1915 to 1949 and 2005 to 2013). This indicates that the multi-decadal variation of the relative abundance of the minerals can be attributed to the local temperature changes in Greenland. The trajectory analysis showed that the air mass arriving at the SIGMA-D site came mainly from the western coast of Greenland from 1958 to 2013 and the contribution showed little inter-annual variabilities, indicating that the variations in the geological origins of the ice core dust were unlikely due to changes in air mass transportation. The abundant minerals in the two warming periods were probably due to an increase of dust sourced from local ice-free areas because the snow/ice cover duration in the Greenland coastal region was shortened by the recent warming during the melt season. On the other hand, the abundant kaolinite in the cooling period was likely derived from old sediments at higher latitudes from North America, rather than from low and middle latitudes. Although further analyses are needed to identify the cause of inter-decadal variations in ice core dust, our study is the first to demonstrate a high-temporal-resolution record of mineral composition in a Greenland ice core over the past 100 years.

https://doi.org/10.5194/cp-2020-146
Preprint. Discussion started: 3 December 2020

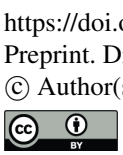

Climate of the Past Discussions
Open Access
EGU

Appendix A: Figures

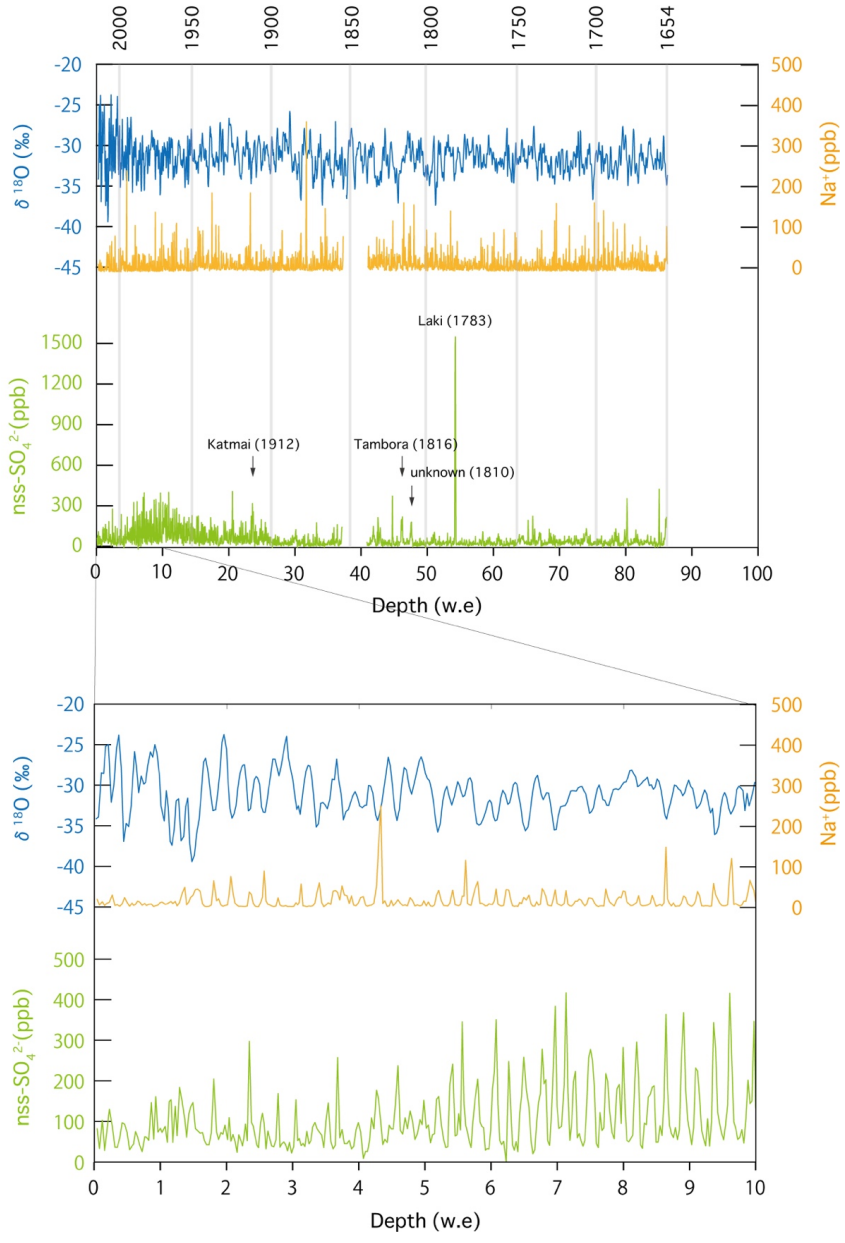

Figure A1. ^{18}O, Na^+, and nss SO_4^{2-} records in the upper 112.87m (86.06m w.e.) of the SIGMA-D ice core. Major volcanic signals we identified are shown in SO_4^{2-} record. Bottom plots shows the enlarged record from 0 to 10 m w.e.

https://doi.org/10.5194/cp-2020-146
Preprint. Discussion started: 3 December 2020

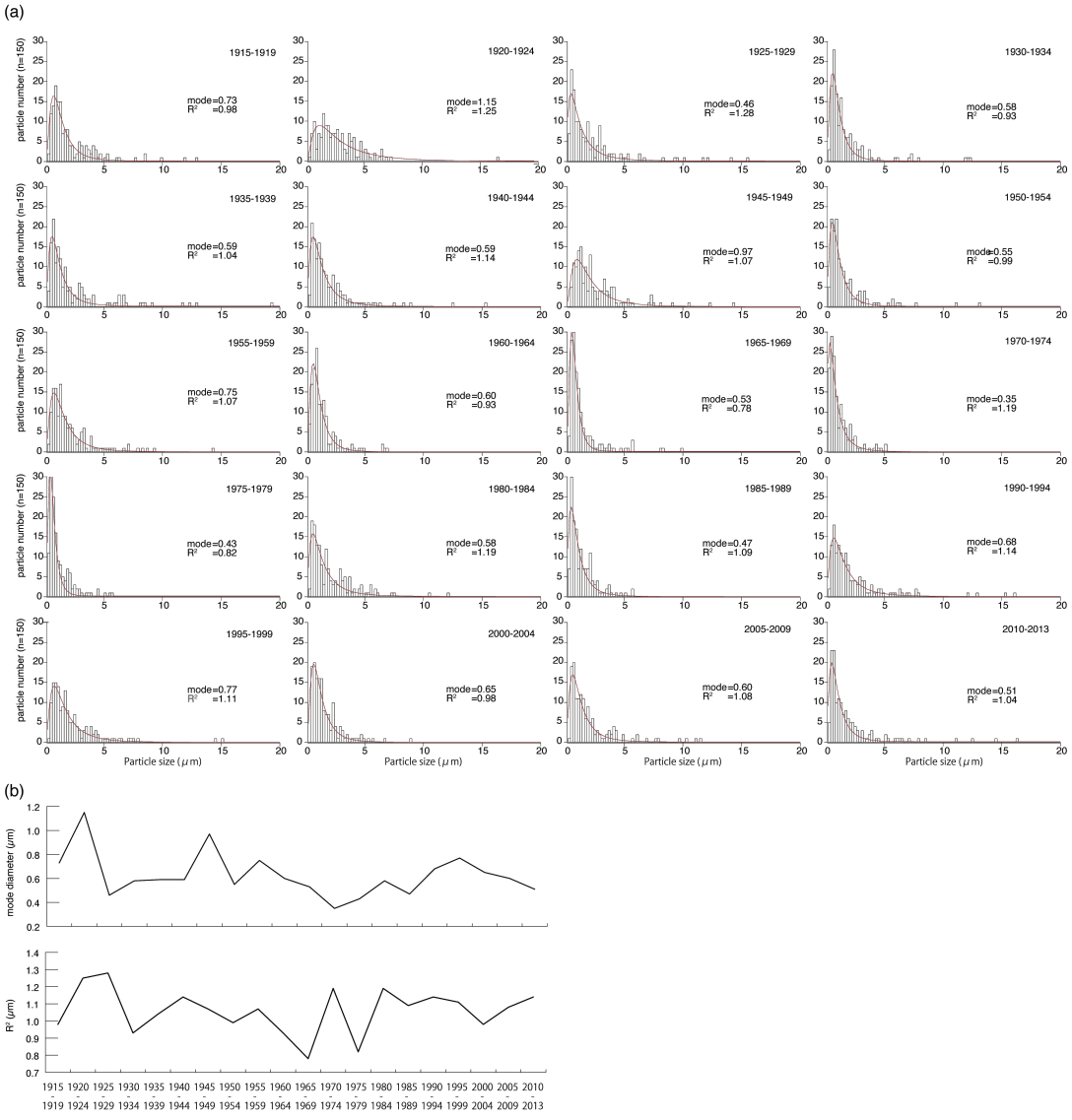

Figure A2. (a) Comparison of particle size distribution and log-normal fitting results (mode: mode diameter and R^2: half peak width) of the ice core minerals among the samples. (b) Historical changes in the mode diameter and R^2

https://doi.org/10.5194/cp-2020-146
Preprint. Discussion started: 3 December 2020

Climate of the Past Discussions

Data availability

Datasets used in this study are available at the following DOIs.

MIROC6 model output prepared for CMIP6 LS3MIP experiments:

https://doi.org/10.22033/ESGF/CMIP6.5622 (land-hist: Onuma and Kim, 2020a).

https://doi.org/10.22033/ESGF/CMIP6.5627 (land-hist-cruNcep : Onuma and Kim, 2020b)

https://doi.org/10.22033/ESGF/CMIP6.5628 (land-hist-princeton: Onuma and Kim, 2020c)

https://doi.org/10.22033/ESGF/CMIP6.5629 (land-hist-wfdei: Onuma and Kim, 2020d)

$\delta^{18}O$ and the concentrations of sodium and sulfate ions (Na^+ and SO_4^{2-}) data will be submitted to the ADS (Arctic Data archive System) database for public use in further analysis.

Authors contribution

NN designed the study and carried out the ice core dust analysis, and wrote the manuscript with help of KGA and KF. KF, SM, YO, YK, MM, HM drilled the ice core. AT, SM, MK obtained ion concentration and water isotope data. NN, AT, KF, SM, MK analyzed the chronology of the ice core. KF conducted the back trajectory analysis. YO conducted the CMIP6 model analysis. TA initiated the project. All authors discussed and commented on the paper.

Competing interests. The authors declare that they have no conflict of interests.

Acknowledgements

We would like to thank Tetsuhide Yamasaki for general fieldwork support. This research was funded by a Grant-in-Aid for JSPS Fellows, by JSPS KAKENHI Grant Numbers 23221004 and 16H01772 (SIGMA Project), and 15K16120, 16J08380, 18H04140, and 19K20443. This study was also supported by the Arctic Challenge for Sustainability (ArCS) grant number JPMXD130000000; the Arctic Challenge for Sustainability II (ArCS II) grant number JPMXD1420318865; the Environment Research and Technology Development Fund (JPMEERF20172003 and JPMEERF20202003) of the Environmental Restoration and Conservation Agency of Japan; and a grant for National Institute of Polar Research, Japan (Project Research KP305).

References

Allen, V. T. and Johns, W. D.: Clays and clay minerals of New England and Eastern Canada, Bull. Geol. Soc. Am., 71 (1), 75–86, https://doi.org/10.1130/0016-7606(1960)71[75:CACMON]2.0.CO;2, 1960.

Amino, T., Iizuka, Y., Matoba, S., Shimada, R., Oshima, N., Suzuki, T., Ando, T., Aoki, T., and Fujita, K.: Increasing dust emission from ice free terrain in southeastern Greenland since 2000, Polar Science, https://doi.org/10.1016/j.polar.2020.100599, (in press).

Bergaya, F., Theng, B. K. G., and Legaly, G. (Eds.): Handbook of Clay Science. Development in Clay Science, Elsevier, Amsterdam., 2006.

Biscaye, P. E.: Mineralogy and sedimentation of recent deep-sea clay in the Atlantic Ocean and adjacent seas and oceans, Geol. Soc. Am. Bull., 76, 803–832, https://doi.org/10.1130/0016-7606(1965)76[803:MASORD]2.0.CO;2, 1965

Biscaye, P. E., Grousset, F. E., Revel, M., Van der Gaast, S., Zielinski, G. A., Vaars, A., and Kukla, G.: Asian provenance of glacial dust (stage 2) in the Greenland Ice Sheet Project 2 ice core, Summit, Greenland, J. Geophys. Res., 102, 26765–26781, https://doi.org/10.1029/97JC01249, 1997.

https://doi.org/10.5194/cp-2020-146
Preprint. Discussion started: 3 December 2020

Bendixen, M., Iversen, L. L., Bjørk, A. A., Elberling, B., Westergaard-Nielsen, A., Overeem, I., Barnhart, K. R., Khan, S. A., Box, J. E., Abermann, J.: Delta progradation in Greenland driven by increasing glacial mass loss, Nature., 550, 101–104. https://doi.org/10.1038/nature23873, 2017.

Box, J. E. and Herrington, A.: Was there a 1930's meltdown of Greenland glaciers?, American Geophysical Union Fall Meeting, San Francisco, USA, 10–14 December 2007, C11A-0077, 2007.

Box, J. E., Yang, L., Bromwich, D. H,. and Bai, L.: Greenland Ice Sheet Surface Air Temperature Variability: 1840–2007., J. Climate, 22, 4029–4049, https://doi.org/10.1175/2009JCLI2816, 2009.

Bullard, J. E. and Austin, M. J.: Dust generation on a proglacial floodplain, West Greenland, Aeolian Res., 3, 43–54, https://doi.org/10.1016/j.aeolia.2011.01.002, 2011.

Bullard, J. E., and Mockford, T.: Seasonal and decadal variability of dust observations in the Kangerlussuaq area, west Greenland, Arct. Antarct. Alp. Res., 50:1, https://doi.org/10.1080/15230430.2017.1415854, 2018.

Cappelen, J. (ed): Denmark - DMI Historical Climate Data Collection 1768-2018, DMI Report 19-02, Copenhagen, 2019

Clausen, H. B. and Hammer, C. U.: The Laki and Tambora eruptions as revealed in Greenland ice cores from 11 locations, Ann. Glaciol., 10, 16–22, https://doi.org/10.3189/S0260305500004092, 1988.

Cremaschi, M., Paleosols and Ventusols in the Central Po Plain (Northern Italy), A Study in Quaternary Geology and Soil Development, Unicopli, Milano, Italy, 1987.

Darby, D. A.: Kaolinite and other clay minerals in Arctic Ocean sediments, J. Sediment. Petrol., 45, 272–279, https://doi.org/10.1306/212F6D34-2B24-11D7-8648000102C1865D, 1975.

De Angelis, M., Steffensen, J. P., Legrand, M., Clausen, H., and Hammer, C.: Primary aerosol (sea salt and soil dust) deposited in Greenland ice during the last climatic cycle: Comparison with East Antarctic records, J. Geophys. Res., 102, 26681–26698, https://doi.org/10.1029/97JC01298, 1997.

Dee, D. P., Uppala, S. M., Simmons, A. J., Berrisford, P., Poli, P., Kobayashi, S., and Vitart, F.: The ERA-Interim reanalysis: Configuration and performance of the data assimilation system, Quart. J. Royal Meteorol. Soc., 137, 553–597, https://doi.org/10.1002/qj.828, 2011.

Deer, F. R. S., Howie, R. A., and Zussman, J.: An Introduction to the Rock-Forming Minerals, Longman, White Plains, New York, USA, 1993.

Devi, S., Bijaksana, S., Fajar, S. J., and Santoso, N. A.: Characterization of Volcanic Ash From the 2017 Agung Eruption, Bali, Indonesia, IOP Conf. Series: Earth and Environmental Science, 318, 012014, https://doi.org/10.1088/1755-1315/318/1/012014, 2019.

Donarummo, J., Ram, M., and Stoermer, E. F.: Possible deposit of soil dust from the 1930's U.S. dust bowl identified in Greenland ice, Geophys. Res. Lett., 30(6), 1269, https://doi.org/10.1029/2002GL016641, 2003.

Drab, E., Gaudichet, A., and Jaffrezo, J. L.: Mineral particles content in recent snow at Summit (Greenland). Atmospheric Environment., 36, 5365–5367, https://doi.org/10.1016/S1352-2310(02)00470-3, 2002.

Eyring, V., Bony, S., Meehl, G. A., Senior, C. A., Stevens, B., Stouffer, R. J., and Taylor, K. E.: Overview of the Coupled Model Intercomparison Project Phase 6 (CMIP6) experimental design and organization, Geosci. Model Dev., 9, 1937–1958, https://doi.org/10.5194/gmd-9-1937-2016, 2016.

Fuhrer, K., Wolff, E. W., and Johnsen, S. J.: Timescales for dust variability in the Greenland Ice Core Project (GRIP) ice core in the last 100,000 years, J. Geophys. Res., 104 (D24), 31043– 31052, https://doi.org/10.1029/1999JD900929, 1999.

Genthon, C. and Armengaud, A.: GCM simulations of atmospheric tracers in the polar latitudes: South Pole (Antarctica) and Summit (Greenland) cases, Sci. Total Environ., 160/161, 101–116, https://doi.org/10.1016/0048-9697(95)04348-5, 1995.

Griffin, J. J., Windom, H., and Goldberg, E. D.: The distribution of clay minerals in the world ocean, Deep Sea Res. Oceanogr., 15, 433–459, https://doi.org/10.1016/0011-7471(68)90051-X, 1968.

https://doi.org/10.5194/cp-2020-146
Preprint. Discussion started: 3 December 2020

Grumet, N. S., Wake, C. P., Zielinski, G., Fisher, D. A., Koerner, R. M., and Jacobs, J. D.: Preservation of glaciochemical time-series in snow and ice from Penny Ice Cap, Baffin Island, Geophys. Res. Lett., 25, 357–360, https://doi.org/10.1029/97GL03787, 1998.

Hanna, E., Fettweis, X., Mernild, S. H., Cappelen, J., Ribergaard, M. H., Shuman, C. A., Steffen, K., Wood, L., and Mote, T.L.: Atmospheric and oceanic climate forcing of the exceptional Greenland ice sheet surface melt in summer 2012, Int. J. Climatol., 34, 1022–1037, https://doi.org/10.1002/joc.3743, 2014.

Harris, I. C.: CRU JRA v2.0: A forcings dataset of gridded land surface blend of Climatic Research Unit (CRU) and Japanese reanalysis (JRA) data; Jan.1901 - Dec. 2018., Centre for Environmental Data Analysis, https://catalogue.ceda.ac.uk/uuid/7f785c0e80aa4df2b39d068ce7351bbb, 2019.

Hurrell, J. and National Center for Atmospheric Research Staff (Eds), The Climate Data Guide: Hurrell North Atlantic Oscillation (NAO) Index (station-based), Retrieved from https://climatedataguide.ucar.edu/climate-data/hurrell-north-atlantic-oscillation-nao-index-station-based, Last modified: 24 Apr 2020.

Iizuka, Y., Uemura, R., Fujita, K., Hattori, S., Seki, O., Miyamoto, C., Suzuki, T., Yoshida, N., Motoyama, H. and Matoba, S.: A 60 year record of atmospheric aerosol depositions preserved in a high-accumulation dome ice core, Southeast Greenland, J. Geophys. Res., 123, 574–589. https://doi.org/10.1002/2017JD026733, 2018.

Ito, A. and Wagai, R.: Global distribution of clay-size minerals on land surface for biogeochemical and climatological studies, Sci. Data., 4, 170103, https://doi.org/10.1038/sdata.2017.103, 2017.

Kemp, S. J., Ellis, M. A., Mounteney, I., and Kender, S.: Palaeoclimatic implications of high-resolution clay mineral assemblages preceding and across the onset of the Palaeocene–Eocene thermal maximum, North Sea Basin, Clay Minerals, 51, 793–813, https://doi.org/10.1180/claymin.2016.051.5.08, 2016.

Kim, H.: Global Soil Wetness Project Phase 3 Atmospheric Boundary Conditions (Experiment 1), Data Integration and Analysis System (DIAS), https://doi.org/10.20783/DIAS.501, 2017.

Kobashi, T., Kawamura, K., Severinghaus, J. P., Barnola, J.-M., Nakaegawa, T., Vinther, B. M., Johnsen, S. J., and Box, J. E.: High variability of Greenland surface temperature over the past 4000 years estimated from trapped air in an ice core, Geophys. Res. Lett., 38, L21501, https://doi.org/10.1029/2011GL049444, 2011.

Koide, M., Michel, R., Goldberg, E., Herron, M. M., and Langway, C. C.: Characterization of radioactive fallout from pre- and post-moratorium tests to polar ice caps. Nature, 296, 544–547, https://doi.org/10.1038/296544a0, 1982.

Kuramoto, T., Goto-Azuma, K., Hirabayashi, M., Miyake, T., Motoyama, H., Dahl-Jensen, D., and Steffensen, J. P.: Seasonal variations of snow chemistry at NEEM, Greenland. Ann. Glaciol., 52(58), 193–200, https://doi.org/10.3189/172756411797252365, 2011.

Kurosaki, Y. and Mikami, M.: Recent frequent dust events and their relation to surface wind in East Asia. Geophys. Res. Lett., 30 (14), 1736, https://doi.org/10.1029/2003GL017261, 2003.

Kurosaki, Y., Matoba, S., Iizuka, Y., Niwano, M., Tanikawa, T., Ando, T., Hori, A., Miyamoto, A., Fujita, S., and Aoki, T.: Reconstruction of sea ice concentration in northern Baffin Bay using deuterium excess in a coastal ice core from the northwestern Greenland Ice Sheet, J. Geophys. Res. Atmos., 125, e2019JD031668, https://doi.org/10.1029/2019JD031668, 2020.

Legrand, M. and Mayewski, P.: Glaciochemistry of polar ice cores: A review, Rev. Geophys., 35(3), 219–243, https://doi.org/10.1029/96RG03527, 1997.

Lupker, M., Aciego, S. M., Bourdon, B., Schwander, J., and Stocker, T. F.: Isotopic tracing (Sr, Nd, U and Hf) of continental and marine aerosols in an 18th century section of the Dye-3 ice core (Greenland), Earth Planet. Sci. Lett., 295, 277–286, https://doi.org/10.1016/j.epsl.2010.04.010, 2010.

Maggi, V.: Mineralogy of atmospheric microparticles deposited along the Greenland Ice Core Project ice core, J. Geophys. Res., 102, 26725–26734, https://doi.org/10.1029/97JC00613, 1997.

https://doi.org/10.5194/cp-2020-146
Preprint. Discussion started: 3 December 2020

480 Matoba, S., Narita, H., Motoyama, H., Kamiyama, K., and Watanabe, O.: Ice core chemistry of Vestfonna Ice Cap in Svalbard, Norway, J. Geophys. Res., 107(D23), 4721, https://doi.org/10.1029/2002JD002205, 2002.

Matoba, T., Motoyama, H., Fujita, K., Yamasaki, T., Minowa, M., Onuma, Y., Komuro, Y., Aoki, T., Yamaguchi, S., Sugiyama, S., and Enomoto, H.: Glaciological and meteorological observations at the SIGMA-D site, northwestern Greenland Ice Sheet. Bull. Glaciol. Res., 33, 7–14, https://doi.org/10.5331/bgr.33.7, 2015.

485 Mayewski, P. A., Meeker, L. D., Twickler, M. S., Whitlow, S., Yang, Q., Lyons, W. B., and Prentice, M.: Major features and forcing of high-latitude northern hemisphere atmospheric circulation using a 110,000-year-long glaciochemical series, J. Geophys. Res., 102(C12), 26345–26366, https://doi.org/10.1029/96JC03365, 1997.

Mudroch, A., Zeman, A. J., and San, R.: Identification of mineral particles in fine grained lacustrine sediments with transmission electron microscope and x-ray energy dispersive spectroscopy, J. Sedimentol. Petrol., 47(1), 244–250,
490 https://doi.org/10.1306/212F713F-2B24-11D7-8648000102C1865D, 1977.

Mueller, J. P. and Bocquier, G.: Dissolution of kaolinites and accumulation of iron oxides in lateritic-ferruginous nodules: Mineralogical and microstructural transformations, Geoderma, 37, 113-116, https://doi.org/10.1016/0016-7061(86)90025-X, 1986.

Nagatsuka, N., Takeuchi, N., Uetake, J. and Shimada, R.: Mineralogical composition of cryoconite on glaciers in northwest
495 Greenland, Bull. Glaciol. Res, 32, 107–114, https://doi.org/10.5331/bgr.32.107, 2014.

Nahon, D. B.: Introduction to the Petrology of Soils and Chemical Weathering, John Wiley, New York, 1991.

Onuma, Y. and Kim, H.: MIROC6 model output prepared for CMIP6 LS3MIP land-hist, Version 20200423, Earth System Grid Federation, https://doi.org/10.22033/ESGF/CMIP6.5622, 2020a.

Onuma, Y. and Kim, H.: MIROC6 model output prepared for CMIP6 LS3MIP land-hist-cruNcep, Version 20200918, Earth
500 System Grid Federation, https://doi.org/10.22033/ESGF/CMIP6.5627, 2020b.

Onuma, Y. and Kim, H.: MIROC6 model output prepared for CMIP6 LS3MIP land-hist-princeton, Version 20200918, Earth System Grid Federation, https://doi.org/10.22033/ESGF/CMIP6.5628, 2020c.

Onuma, Y. and Kim, H.: MIROC6 model output prepared for CMIP6 LS3MIP land-hist-wfdei, Version 20200727, Earth System Grid Federation, https://doi.org/10.22033/ESGF/CMIP6.5629, 2020d.

505 Oyabu, I., Matoba, S., Yamasaki, T., Kadota, M. and Iizuka, Y.: Seasonal variations in the major chemical species of snow at the South East Dome in Greenland, Polar Sci., 10, 36–42, https://doi.org/10.1016/j.polar.2016.01.003, 2016.

Pallister, J. S., Hoblitt, R. P., and Reyes, A. G.: A basalt trigger for the 1991 eruptions of Pinatubo volcano?, Nature., 356, 426–428, https://doi.org/10.1038/356426a0, 1992.

Parvin, F., Seki, O. Fujita, K., Iizuka, Y., Matoba, S. and Ando, T.: Assessment for paleoclimatic utility of biomass burning
510 tracers in SE-Dome ice core, Greenland, Atmos. Environ., 196, 86–94, https://doi.org/10.1016/j.atmosenv.2018.10.012, 2018.

Pye, K.: Aeolian Dust and Dust Deposits, Academic, San Diego, USA, 1987.

Rex, R. W. and Goldberg, E. D.: Quartz contents of pelagic sediments of the Pacific Ocean, Tellus, 1, 153–159, https://doi.org/10.3402/tellusa.v10i1.9223, 1958.

515 Schüpbach, S., Fischer, H., Bigler, M., Erhardt, T., Gfeller, G., Leuenberger, D., Mini, O., Mulvaney, R., Abram, N. J., Fleet, L., Frey, M. M., Thomas, E., Svensson, A., Dahl-Jensen, D., Kettner, E., Kjaer, H., Seierstad, I., Steffensen, J. P., Rasmussen, S. O., Vallelonga, P., Winstrup, M., Wegner, A., Twarloh, B., Wolff, K., Schmidt, K., Goto-Azuma, K., Kuramoto, T., Hirabayashi, M., Uetake, J., Zheng, J., Bourgeois, J., Fisher, D., Zhiheng, D., Xiao, C., Legrand, M., Spolaor, A., Gabrieli, J., Barbante, C., Kang, J.-H., Hur, S. D., Hong, S. B., Hwang, H. J., Hong, S., Hansson, M., Iizuka, Y., Oyabu,
520 I., Muscheler, R., Adolphi, F., Maselli, O., McConnell J., and Wolff, E. W.: Greenland records of aerosol source and atmospheric lifetime changes from the Eemian to the Holocene, Nat. Commun., 9, 1476, https://doi.org/10.1038/s41467-018-03924-3, 2018.

https://doi.org/10.5194/cp-2020-146
Preprint. Discussion started: 3 December 2020

Severin, K. P.: Energy dispersive spectrometry of common rock forming minerals, Kluwer Academic Publishers, Dordrecht, the Netherlands, 2004.

Sheffield, J., Goteti, G., and Wood, E. F.: Development of a 50-Year High-Resolution Global Dataset of Meteorological Forcings for Land Surface Modeling, J. Climate, 19, 3088–3111, https://doi.org/10.1175/JCLI3790.1, 2006.

Steffensen, J.: The size distribution of microparticles from selected segments of the Greenland Ice Core Project ice core representing different climatic periods. J. Geophys. Res., 102, 26755–26763, https://doi.org/10.1029/97JC01490, 1997.

Stein, A. F., Draxler, R. R., Rolph, G. D., Stunder, B. J. B., Cohen, M. D., and Ngan, F.: NOAA's HYSPLIT Atmospheric Transport and Dispersion Modeling System, Bull. Am. Meteorol. Soc., 96(12), 2059–2077, https://doi.org/10.1175/BAMS-D-14-00110.1, 2015.

Svensson, A., Biscaye, P. E., and Grousset, F. E.: Characterization of late glacial continental dust in the greenland ice core project ice core, J. Geophys. Res., 105 (D4), 4637–4656, https://doi.org/10.1029/1999JD901093, 2000.

Tatebe, H., Ogura, T., Nitta, T., Komuro, Y., Ogochi, K., Takemura, T., Sudo, K., Sekiguchi, M., Abe, M, Saito, F., Chikira, M., Watanabe, S, Mori, M, Hirota, N, Kawatani, Y., Mochizuki, T., Yoshimura, K., Takata, K., O'ishi, R., Yamazaki, D., Suzuki, T., Kurogi, M., Kataoka, T., Watanabe, M., and Kimoto, M.: Description and basic evaluation of simulated mean state, internal variability, and climate sensitivity in MIROC6, Geosci Model Dev., 12, 2727–2765, https://doi.org/10.5194/gmd-12-2727-2019, 2019.

Taylor, H. E. and Lichte, F. E.: Chemical composition of Mount St. Helens volcanic ash, Geophys. Res. Lett., 7, 949–952, https://doi.org/10.1029/GL007i011p00949, 1980.

Uppala, S. M., Kallberg, P. W., Simmons, A. J., Andrae, U., daCosta Bechtold, V., Fiorino, M., Gibson, J. K., Haseler, J., Hernandez, A., Kelly, G. A., Li, X., Onogi, K., Saarinen, S., Sokka, N., Allan, R. P., Andersson, E., Arpe, K., Balmaseda, M. A., Beljaars, A. C. M., van de Berg, L., Bidlot, J., Bormann, N., Caires, S., Chevallier, F., Dethof, A., Dragosavac, M., Fisher, M., Fuentes, M., Hagemann, S., Holm, E., Hoskins, B. J., Isaksen, L., Janssen, P. A. E. M., Jenne, R., McNally, A. P., Mahfouf, J. F., Morcrette, J. J., Rayner, N. A., Saunders, R. W., Simon, P., Sterl, A., Trenberth, K. E., Untech, A., Vasiljevic, D., Viterbo, P., and Woollen, J.: The ERA-40 Reanalysis, Quart. J. Roy. Meteor. Soc., 131 (612), 2961–3012, https://doi.org/10.1256/qj.04.176, 2005.

van den Broeke, M., Bamber, M. J., Ettema, J., Rignot, E., Schrama, E., van de Berg, W. J., van Meijgaard, E., Velicogna, I. and Wouters, B.: Partitioning recent Greenland mass loss. Science, 326, 984–986, https://doi.org/10.1126/science.1178176, 2009.

van den Hurk, B., Kim, H., Krinner, G., Seneviratne, S. I., Derksen, C., Oki, T., Douville, H., Colin, J., Ducharne, A., Cheruy, F., Viovy, N., Puma, M.J., Wada, Y., Li, W., Jia, B., Alessandri, A., Lawrence, D.M., Weedon, G.P., Ellis, R., Hagemann, S., Mao, J., Flanner, M.G., Zampieri, M., Materia, S., Law, R. M. and Sheffield, J.: LS3MIP (v1.0) contribution to CMIP6: the Land Surface, Snow and Soil moisture Model Intercomparison Project – aims, setup and expected outcome, Geosci. Model Dev., 9, 2809–2832, https://doi.org/10.5194/gmd-9-2809-2016, 2016.

Velde, B.: Origin and Mineralogy of Clays: Clays and Environment, Springer-Verlag, New York, 1995.

Weedon, G. P., Balsamo, G., Bellouin, N., Gomes, S., Best, M. J., and Viterbo, P.: The WFDEI meteorological forcing data set: WATCH Forcing Data methodology applied to ERA Interim reanalysis data, Water Resour. Res., 50, 7505–7514, https://doi.org/10.1002/2014WR015638, 2014.

Whitlow, S., Mayewski, P. A., and Dibb, J. E.: A comparison of major chemical species seasonal concentration and accumulation at the South Pole and Summit, Greenland, Atmos. Environ., 26A(11), 2045–2054, https://doi.org/10.1016/0960-1686(92)90089-4, 1992.

Wilson, T. R. S.: Salinity and the major elements of sea water. Chemical Oceanography, 2nd Edition, Vol. 1., edited by: Riley, J.P. and Skirrow, G., Academic Press, Orland, 365–413, 1975.

https://doi.org/10.5194/cp-2020-146
Preprint. Discussion started: 3 December 2020

565 Woollings, T., Hannachi, A., Hoskins, B., and Turner, A.: A regime view of the North Atlantic Oscillation and its response to anthropogenic forcing, J. Clim., 23, 1291–1307, https://doi.org/10.1175/2009JCLI3087.1, 2010.

Wu, G., Zhang, X., Zhang, C., and Xu, T.: Mineralogical and morphological properties of individual dust particles in ice cores from the Tibetan Plateau, J. Glaciol., 62 (231), 46–53, https://doi.org/10.1017/jog.2016.8, 2016.

Yokoo, Y., Nakano, T., Nishikawa, M., and Quan, H.: Mineralogical variation of Sr—Nd isotopic and elemental compositions
570 in loess and desert sand from the central Loess Plateau in China as a provenance tracer of wet and dry deposition in the northwestern Pacific, Chem. Geol., 204, 45–62, https://doi.org/10.1016/j.chemgeo.2003.11.004, 2004.